OPEN ACCESS



Interplanetary Signatures during the 1972 Early August Solar Storms

Consuelo Cid¹, Elena Saiz¹, Manuel Flores-Soriano¹, and Delores J. Knipp^{2,3}

Space Weather Research Group, Departamento de Física y Matemáticas, Universidad de Alcalá, Alcalá de Henares, Madrid, Spain; consuelo.cid@uah.es

Smead Aerospace Engineering Sciences Department, University of Colorado Boulder, CO USA

Space Weather Technology Research and Education Center, University of Colorado Boulder, CO USA

Received 2023 August 2; revised 2023 September 13; accepted 2023 September 13; published 2023 November 21

Abstract

In 1972, early August, a series of interplanetary shocks were observed in the heliosphere from 0.8 to 2.2 au. These shocks were attributed to a series of brilliant flares and plasma clouds since at that time coronal mass ejections (CMEs) and their interplanetary counterparts (ICMEs) were unknown to the scientific community. This paper aims to reinterpret the interplanetary data in light of the current understanding about interplanetary transients and to track the evolution of the ICMEs, taking advantage of the alignment of Pioneers 9 and 10 spacecraft. For this purpose, we reanalyze in situ data from these two Pioneers and also from Heos, Prognoz 1 and 2, and Explorer 41 spacecraft searching for ICMEs and high-speed streams. Then we assemble the interplanetary transients and solar activity and analyze the propagation of the ejections through the heliosphere. The evolution of four ICMEs and a high-speed stream from a low-latitude coronal hole is followed using the multipoint in situ observations. The first three ICMEs show clear signatures of ICME–ICME interaction in the interplanetary medium, suggesting the first observations of an ICME which developed into an ICME-in-the-sheath. For a non-perturbed ICME event, we obtain the evolution parameter, ζ , related to the local expansion of ICMEs, getting similar values for Pioneer 9 (ζ = 0.80) and Pioneer 10 (ζ = 0.78). These results support previous findings of ζ being independent of the heliocentric distance and the magnetic field strength decreasing as $r^{-2}\zeta$.

Unified Astronomy Thesaurus concepts: Solar activity (1475); Interplanetary shocks (829); Solar flares (1496); Solar coronal mass ejections (310)

1. Introduction

On 1972 August 2–7, McMath Region (MR) 11976 produced a series of brilliant flares. The events were extensively analyzed by the scientific community in the 1970s and 1980s due to their relevance considering the enhanced levels of solar activity. At that time, flares were considered to be a source of interplanetary (IP) shocks. Although coronal mass ejections (CMEs) and their IP counterparts (ICMEs) were still unknown, studies of the 1972 August event began to use terms like "plasma transients" (Croft 1973), "plasma clouds" (Lockwood et al. 1975), and "plasma pistons" (Smith 1976) to describe the disturbances behind shocks.

By the mid-1970s the idea of interacting shocks was widely discussed (e.g., Smith et al. 1977; Dryer et al. 1978); however, the idea of interacting ICMEs and shocks interacting with ICMEs is a newer construct (e.g., Liu et al. 2014; Temmer & Nitta 2015; Koehn et al. 2022). In this paper, we put the 1972 August shock and ICME interactions into the recent framework of an ICME trapped between shocks (Liu et al. 2020).

The passage of several IP shocks related to this solar activity was observed in Pioneers 9 and 10 data off of the Sun-Earth line. The location of these spacecraft at 0.78 and 2.2 au heliocentric distance, respectively, and at about 45° eastward of the Sun-Earth line, joint to Prognoz 1, Prognoz 2, Heos 2, and Explorer 41 (IMP-5) satellites in the vicinity of the Earth (Figure 1), was particularly suitable for the study of the evolution of the solar ejections in the heliosphere. Only a few events of ICMEs have been seen at different locations (Möstl

Original content from this work may be used under the terms of the Creative Commons Attribution 4.0 licence. Any further distribution of this work must maintain attribution to the author(s) and the title of the work, journal citation and DOI.

et al. 2012; Salman et al. 2020; Davies et al. 2021; Möstl et al. 2022). The events in 1972 August are one of these examples, providing an excellent opportunity to study its evolution. Therefore, it is time for a reconsideration of available data in line with current knowledge.

Solar wind plasma and magnetic field measurements from Pioneers 9 and 10 during 1972 August 2–17 were first described by Mihalov et al. (1973). They identified the passage of four fast forward IP shocks in Pioneer 9 data and identified the solar flares, which were the source of the four forward shocks (note that at that time CMEs were still unknown). The four flares were from MR 11976, and types II and IV radio emission were detected during all of them (Coffey 1973; Watanabe et al. 1973; Zastenker et al. 1978) as a signature of solar ejections associated with the flaring activity. Dryer et al. (1974) and later Dryer et al. (1975) synthesized the IP shocks related to these four flares, not only from Pioneers 9 and 10 data, but also from Heos 2, Prognoz 1, and Prognoz 2 (Table 1). As in most references quoted in this section, we will use throughout this paper the convention of numbering sequentially the shocks at each location, indicating the location in parentheses. Therefore, S1(9) denotes the first shock observed at Pioneer 9. Also Heos, Prognoz 1 and 2, and Explorer 41 will be considered as measuring at the same location (Earth) and providing a unique data set. Thus Si(E)denotes the ith shock observed at Earth.

Dryer et al. (1975) associated sequentially the four flares to shocks S1(9), S2(9), S3(9), and S4(9) at Pioneer 9 and then to shocks S1(E), S2(E), S3(E), and S4(E) (see lines in Figure 2). At Pioneer 10, they propose S1(10) as the result of the merging of the first three shocks at Earth or at Pioneer 9 and the reverse shock S2(10) as raised due to the interaction of the S3(9) with

 Table 1

 Flares and IP Shocks during 1972 early August (Adapted from Dryer et al. 1975)

Event	I	II	III	IV
Solar Flare				
Time	Aug 2, 03:16 UT	Aug 2, 19:59 UT	Aug 4, 06:21 UT	Aug 7, 15:05 UT
Location	14°N 35°E	13°N 28°E	15°N 09°E	14°N 38°W
$H\alpha$ Importance	1B	2B	2B	3B
IP Shock				
Pioneer 9	Aug 3, 04:40 UT S1(9)	Aug 3, 11:17 UT S2(9)	Aug 4, 23:23 UT S3(9)	Aug 9, 07:10 UT S4(9)
Prognoz 1	Aug 4, 01:18 UT	Aug 4, 02:21 UT	***	•••
Prognoz 2	Aug 4, 01:16 UT	Aug 4, 02:21 UT	Aug 4, 20:46-21:57 UT	Aug 8, 23:52 UT
Heos 2	Aug 4, 01:19 UT	Aug 4, 02:20 UT	Aug 4, 20:54 UT	
	SI(E)	S2(E)	S3(E)	S4(E)
Pioneer 10		•••	Aug 6, 15:06 UT S1(10)	Aug 13, 02:45 UT S3(10)
			Aug 9, 15:26 UT S2(10) R	

Note. All IP shocks are fast forward unless noted as reverse (R).

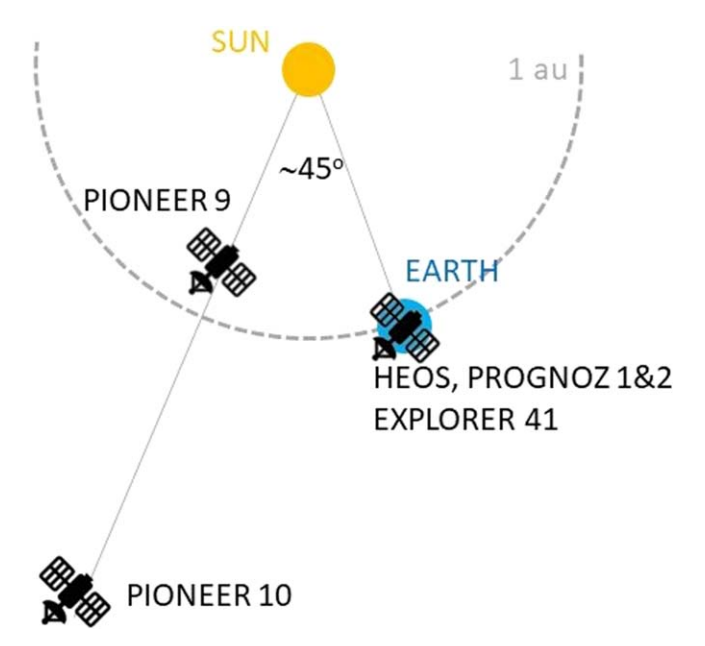


Figure 1. Position of spacecraft in 1972 August in the ecliptic plane.

S2(9). Finally, Dryer et al. (1975) consider S3(10) associated with the fourth flare and also with a high-speed stream.

The proposal that all shocks at Pioneers 9 and 10 and at Earth were related to the corresponding flare was also considered by Intriligator (1976). She agreed with Dryer (1975) about the relationship among the four flares and the four shocks in Pioneer 9 and at Earth sequentially. She also supported the association between S2(9) and S1(10), considering the shock speed of S2(E) calculated by Cattaneo et al. (1974), and agreed with Dryer et al. (1975) that beyond 1 au, S1(9) is overtaken by S2(9) to become S1(10). She also proposed that S4(9) is related to S3(10). Nevertheless, Intriligator (1976) concluded that the association between S3(9) and S1(10) was incorrect, based on the agreement between the local shock speeds S2(9) and S1(10) (about 600 km s⁻¹) and the estimated average shock speed, assuming that shock S2(9) propagated radially outward from Pioneer 9 to Pioneer 10. There was no proposal for the evolution of S3(9)

beyond 1 au or for the source of the reverse shock S2(10) in Intriligator (1976).

Numerical MHD simulations using the observations at 0.8 au from Pioneer 9 as forcing functions (Dryer et al. 1978) supported the overtaking of S1(9) by S2(9) at approximately 1.16 au, before reaching Pioneer 10. This proposal was also supported by Smith et al. (1977). Moreover, Smith et al. (1977) suggested again the possibility that the first three flares gave rise to three forward shocks at Pioneer 9 and at Earth, leading to a single forward shock at Pioneer 10, S1(10). Smith et al. (1977) also identified the reverse shock on August 9 at 15:40 UT in Pioneer 10, S2(10), indicating that it was not observed either at Earth or at Pioneer 9 and suggesting that it must have developed after 1 au. Smith et al. (1977) reported wavelike quasiperiodic variations in both the field direction and the magnitude before the reverse shock.

MHD simulation results in Dryer et al. (1978) confirmed the evolution of the four forward shocks at Pioneer 9 in two forward shocks, S1(10) and S3(10), and one reverse shock, S2(10) at Pioneer 10. Nevertheless, these simulation results did not agree with the arrival time of the shocks at Pioneer 10. Dryer et al. (1978) suggested that the key factor responsible for the arrival time discrepancy was rooted in the geometrical assumption of the propagation as pure spherical expansion. Indeed, Zastenker et al. (1978) proposed a nearly spherical shock waveforms for flares on August 2 and nonspherical shock waveforms for flares on August 4 and 7. The departure from spherical symmetry of all the shocks except for the one related to the first flare was also pointed out by Smith (1976).

Regarding the driver(s) of the shocks, Smith et al. (1977) identified the abrupt jump in the magnetic field in Pioneer 10 on August 6 at \sim 20:30 UT (after S1(10)) as the arrival of a plasma driver, considering that at the same time the temperature dropped abruptly, while the magnetic field magnitude remained enhanced almost a day. This driver is confirmed by the MHD results in Dryer et al. (1978). A review of the evolution of the "flare-generated shock waves" by d'Uston (1982) refers to this driver with the term *ejecta*, wondering about the magnetic topography inside the ejected matter.

After some years without specific papers devoted to the 1972 August solar storms, more recent papers appeared devoted to the ultrafast shock S3(E), associated with the flare that peaked

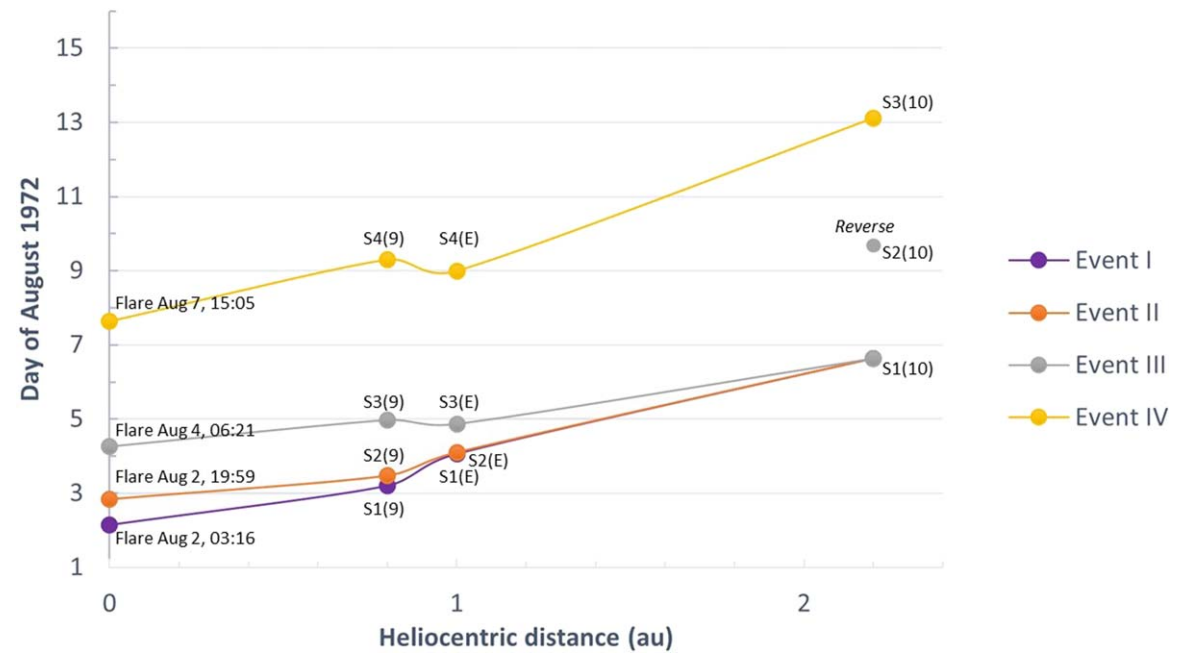


Figure 2. The events observed at different heliocentric distance from the Sun to Pioneer 10 orbit at 2.2 au. Dots correspond to the events in Table 1, and solid lines represent their association according to Dryer et al. (1975).

at 06:21 UT on August 4, driven by an ICME that reached the Earth in less than 15 hr, describing large technological impacts (Cliver et al. 1990; Freed & Russell 2014; Knipp et al. 2018). However, an explanation of the IP signatures observed in early 1972 August, besides the IP shocks, is still missing to date, and it is the purpose of this paper.

2. Identifying in Situ Transients

The detection of type II and IV radio emission during the four flares in 1972 early August (Coffey 1973; Watanabe et al. 1973; Zastenker et al. 1978) guides us to search for the IP counterpart of four CMEs in IP data. The scenario of several CMEs erupting in rather quick succession, running into one another and interacting in the IP medium, anticipates hard-to-find, indubitable signatures of ICMEs including low temperature and enhanced magnetic field strength with the magnetic field vector rotating over a wide angle, as observed, for example, during the passage of a magnetic cloud (Burlaga et al. 1981). Thus, less restrictive conditions will be adopted as fiducials of the ICMEs.

In some cases, an enhanced and smooth magnetic field together with an unexpectedly lower temperature for a time interval of at least 2 hr, following Rouillard et al. (2011), will be enough to identify the ICME. Nevertheless, we do not require lower proton temperature than expected inside the transient as a mandatory signature for ICME identification as interaction between IP structures may enhance this parameter. In some cases, a decreased temperature together with a smooth and enhanced magnetic field will be considered as reliable signatures of an ICME.

Throughout this paper, when we identify an ICME driving a shock, we will label it with the same number of the driven shock at the corresponding spacecraft. For example, ICME1(9) would correspond to the ICME driving the shock, S1(9). Even though we will assemble the IP transients observed by different spacecraft in Section 3, in Figures 3 to 5 we choose a single

identifiable color for each of the ICMEs and use that same color in each graphic to make it easy to follow which of the ICMEs transit from one location to another and which, if any, interact and merge. That way, even if the ICMEs have different numbers at each location, the reader will be aware that we are talking about a long-lasting coherent structure that moves. Besides identifying the four expected ICMEs, our aim also includes the identification of high-speed streams, as a low-latitude coronal hole was following MR 1976 (Watanabe et al. 1973; Kakinuma & Watanabe 1976; Houminer & Hewish 1988). Interplanetary signatures at different spacecraft are analyzed in detail in the following sections. We will start with Pioneer 10, considering the high quality of these data when compared to the other data sets.

2.1. In Situ Data by Pioneer 10

In situ data measured by Pioneer 10 (Figure 3) reveal that ahead of S1(10) on August 6 at 15:06 UT, solar wind conditions were not quiet. Solar wind data for the second half of August 5 and first half of August 6 are clearly disturbed when compared to the first half of August 5: speed changes from \sim 350 to \sim 400, proton temperature is increased by a factor of 3, and density and magnetic field strength are increased by a factor of 2. Then S1(10) arrives, and the fluctuating magnetic field following the shock is associated with a sheath, but fluctuations are reduced in a time interval starting on August 6 \sim 22:15 UT. At that time, the temperature drops (contrary to the enhancement of the speed). The magnetic field vector is less irregular, both in magnitude and direction, and smoothly rotates for about 8 hr with a magnitude over 15 nT, indicating the passage of the ICME1(10), which was already identified as a plasma driver by Smith (1976). Large fluctuations in the magnetic field vector start again on August 7 at \sim 06:15 UT, indicating the end of ICME1(10). A large spike in the density is observed at the rear boundary of this ICME. ICME1(10), like any ICME region in Figures 3 to 5, appears as

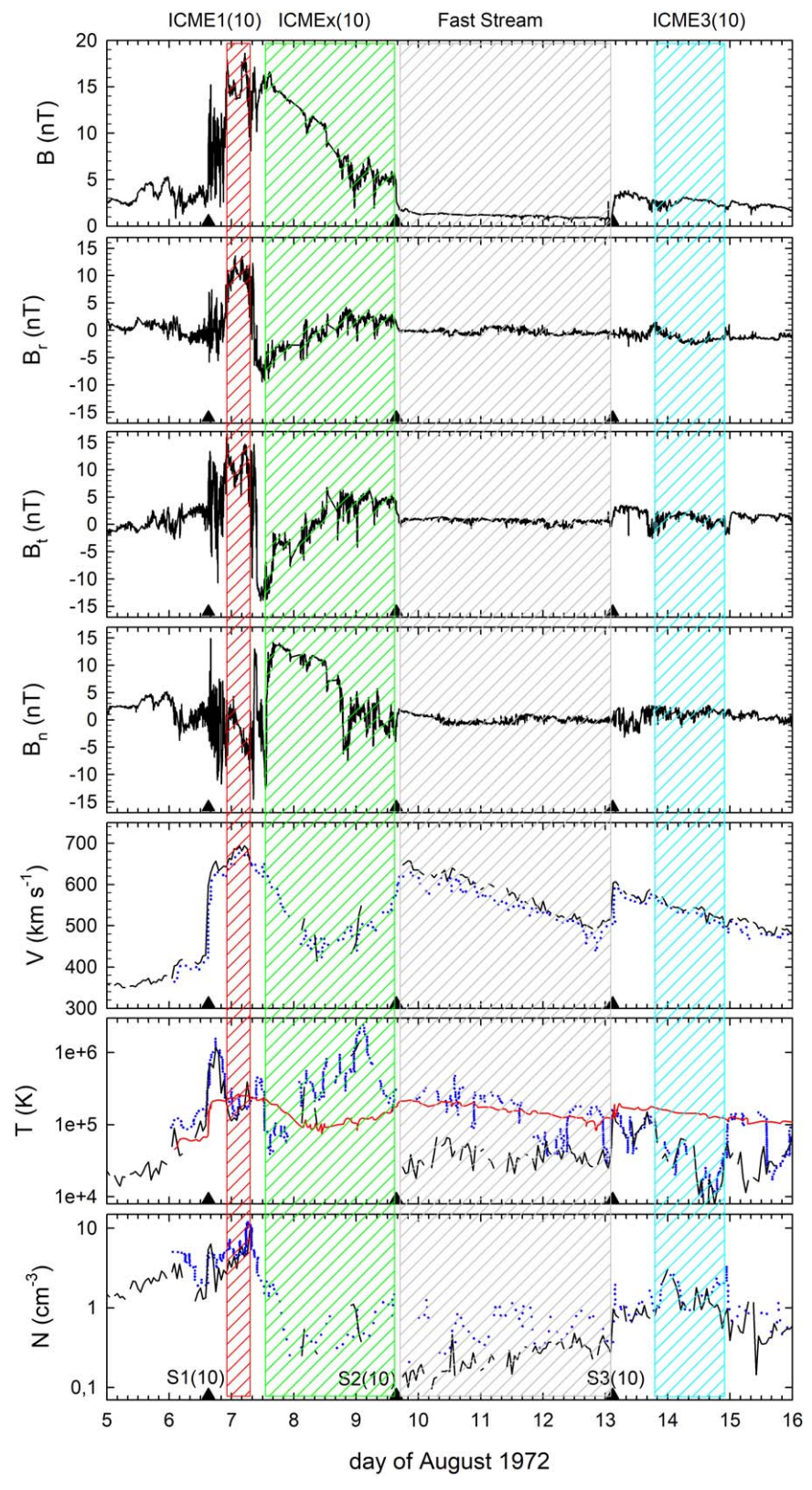


Figure 3. Pioneer 10 IP magnetic field and solar wind plasma measurements during 1972 August 5–16. Solid black lines correspond to 1 minute magnetic field data (strength and RTN components) and hourly plasma data (proton speed, temperature, and density) downloaded from CDAWeb. Plasma data digitized from Figure 1 of Mihalov et al. (1973) are overplotted using the blue dot symbol. Red line in sixth panel corresponds to the expected temperature (Richardson & Cane 1995). The IP shocks of Table 1 appear as black triangles at the bottom of every panel and are labeled in the bottom panel. Colored areas indicate the ICME intervals and the gray shadowed area indicates a high-speed stream region.

a colored area in Figure 3 with the corresponding label at the top of the colored area.

A new drop in temperature on August 7 at \sim 12:30 UT below half of the expected value indicates the front boundary of a new ICME, which will be labeled as ICMEx(10), as it is not driving any shock. This temperature drop combines with a decrease in the density. The rear boundary of ICMEx(10) has been set at the time of the reverse shock S2(10) because until that time the field is large and without waves or discontinuities although the temperature was enhanced before this time. ICMEx(10) region was previously identified as part of a driver gas by Tsurutani et al. (1992).

The reverse shock S2(10) and the forward S3(10) are the boundaries of a region (gray shadowed area) with speed in the range ~450-650 km s⁻¹ and therefore not corresponding to bulk solar wind. The low (\sim 1 nT) and fluctuating magnetic field in this interval are signatures of high-speed streams. Note that in this time interval there is a large discrepancy between temperature data downloaded from CDAWeb-with values around $2-4 \times 10^5$ K—and those digitized from Figure 7 of Mihalov et al. (1973)—with values around $2-4 \times 10^4$ K, unlike any other interval in Figure 3. The temperature values from Mihalov et al. (1973) are consistent with the passage of a highspeed stream where temperature is similar to the expected one from solar wind speed (Richardson & Cane 1995). In any case, the decreased temperature, as observed in data from CDAWeb, and also in Mihalov et al. (1974), is not consistent with the passage of an ICME as the magnetic field strength hardly passes 1 nT. Moreover, Pioneer 10 data one solar rotation ahead of this time interval also detect a high-speed stream preceded by the corresponding interaction region, indicating that the region was indeed a corotating interaction region, definitively associated with the coronal hole following MR 11976. In the following, gray shadowed regions in Figures 3 to 5 will correspond to high-speed streams. Finally, during August 14, we find ICME3(10) from 01:55 to 21:35 UT driving S3(10). The smooth magnetic field and a clearly depressed temperature in that interval are signatures of the passage of an ICME.

2.2. In Situ Data by Pioneer 9

Pioneer 9 magnetic field strength and solar wind plasma data during 1972 August 2–14 are shown in Figure 4. Data have been digitized from Mihalov et al. (1973). The coordinates are the standard solar-ecliptic coordinates with the X-axis (corresponding to a field longitude $\phi=0$) directed toward the Sun, the Z-axis (corresponding to a latitude $\theta=+90^\circ$) pointing toward the north ecliptic pole, and the Y-axis $\phi=90^\circ$ orthogonal to the other two. High-resolution magnetic field and plasma data are also available for several 2 hr intervals in Smith (1976). Considering the data in Figure 4 and the support of the above references, three events fit our criteria for ICMEs (shadowed areas).

The region labeled as ICME2(9), with a depressed temperature while keeping enhanced the magnetic field strength, was already pointed out by Smith (1976) as the driver of S2(9). Ahead of ICME2(9), the large peaks in magnetic field (up to 85 nT) and proton density (about 60 cm $^{-3}$) on August 3 at \sim 12 UT appear as signatures of interaction between the shock S2(9)

and the material ahead of it, which will be the driver of the shock S1(9).

The magnetic field is enhanced up to ~ 10 nT after a data gap early on August 5. During this interval, labeled as ICME3(9), the magnetic field longitude and latitude are also smooth and rotating, contrary to the surrounding more fluctuating field (see Figure 2 in Mihalov et al. 1973). Therefore, although the temperature is not below the expected value at the beginning of the interval, we have considered that this region corresponds to ICME material driving the shock. At the rear boundary of ICME3(9), a sharp decrease in solar wind speed together with an increase in proton temperature, suggests the possibility of a reverse shock-like wave, but the low resolution of the data for this interval does not allow us to be conclusive. Following this reverse wave, Pioneer 9 observations show the passage of a fast ($\sim 400-600~{\rm km~s^{-1}}$) wind, with similar temperature to the expected value and fluctuating magnetic field until S4(9).

Finally, despite the data gap in magnetic field measurements starting on August 10—any of the references in this paper will show the IP magnetic field from August 10 on—the decreased temperature, reaching about one-fourth of the expected value, together with an enhanced magnetic field strength of about 10 nT, indicates the passage of ICME4(9). The decreasing speed profile provides a signature of ICME expansion.

2.3. In Situ Data at Earth

In situ data at Earth during 1972 August 3–13, digitized from d'Uston (1982) and Smith (1976), are shown in Figure 5. Higher-resolution magnetic field vector data at Earth for short intervals are available in some references: from August 4, 21 UT to August 5, 08 UT, measured by Prognoz 1 and 2 in d'Uston et al. (1977); from August 3, 11 UT to August 5, 04 UT, by Heos in Cattaneo et al. (1974); and for the whole day of August 4 in Smith (1976).

The first two shocks at Earth location, S1(E) and S2(E) from Table 1, overlap in Figure 5. The driver of S2(E), ICME2(E), can be identified starting on August 4 at about 4:30 UT. Geomagnetic indices and magnetic pulsation records for August 4 help us to identify a likely magnetic cloud following S2(E), with the interplanetary magnetic field (IMF) predominantly southward from 03:30 to ~06:45 UT on August 4. During this \sim 3 hr interval Dst reached \sim -125 nT. Figure 14 of Smith (1976) shows that from the time of S2(E) to about 4:30 UT, the magnetic field latitude is mostly fluctuating. Such fluctuations are a typical signature of sheath flow following a shock. Apparently the front boundary of the south-field-first ICME2(E) arrives at 4:30 UT on August 4. Thereafter the IMF turns northward and is likely fully northward by 07:30 UT as geomagnetic indices tend to quieter levels. This is supported by a single magnetic field observation at \sim 7 UT that indicates the field in the magnetosheath was northward. We suggest IMF remained northward until S3 (this is partially supported by Figure 14 in Smith 1976). Thus, the short south-field portion of the cloud is followed by a long interval of mostly northward IMF and a recovery phase of the first geomagnetic storm. This ICME is associated with the initial Forbush decrease observed at Mt. Washington and Durham neutron monitors on August 4. As the ICME was passing Earth, a third major solar eruption injected solar energetic particles into the heliosphere. These particles heralded one of the largest solar energetic particle (SEP_ events of the 20th century, one that superposed on the ongoing Forbush decrease. Figure 2 in Lockwood et al. (1975)

https://cdaweb.gsfc.nasa.gov/

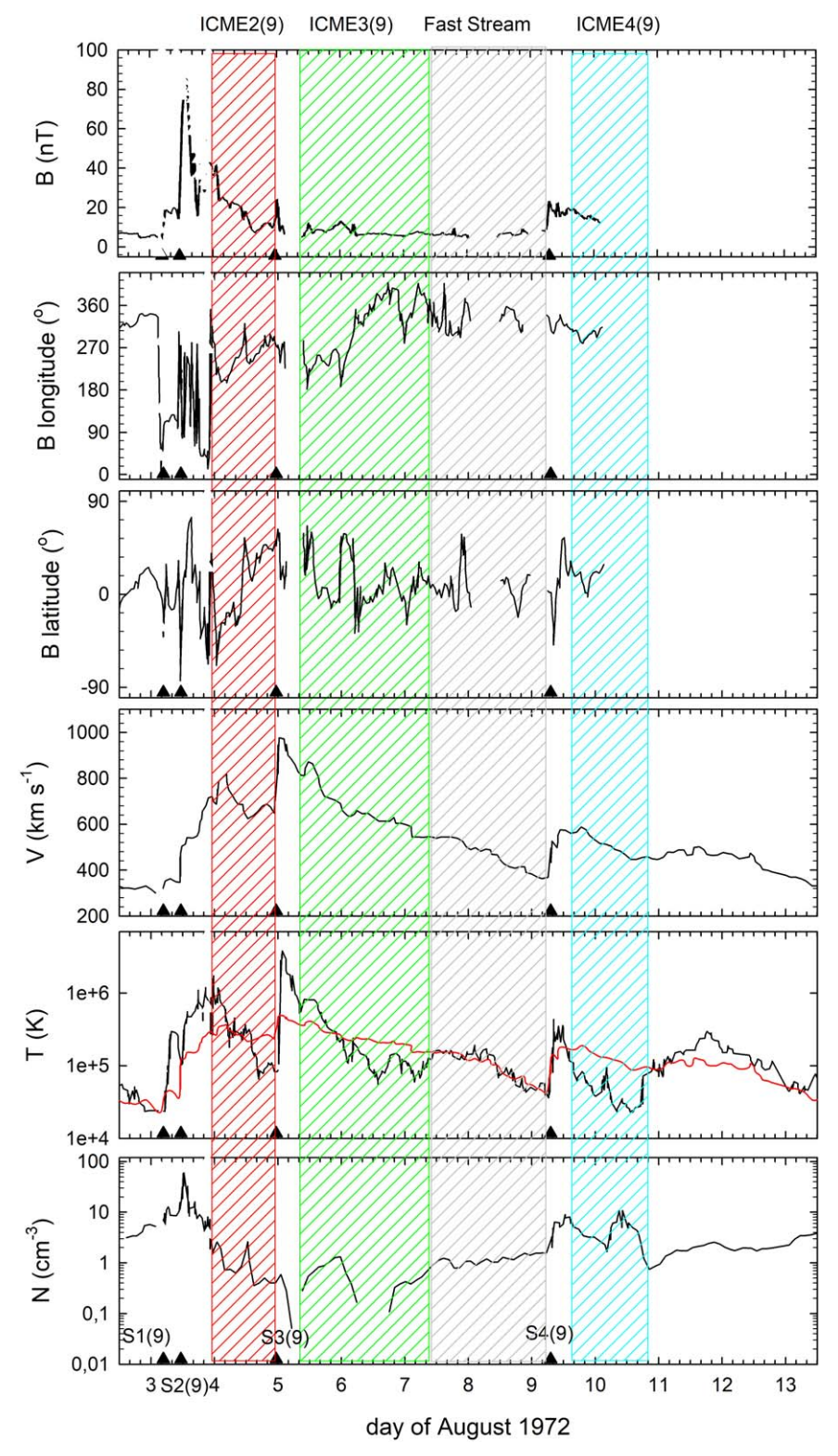


Figure 4. Pioneer 9 IP magnetic field and plasma measurements during 1972 August 2-17 digitized from Figures 1 and 2 of Mihalov et al. (1973).

indicates that only after \sim 12 UT on August 5 did the enhanced solar particles measured by IMP 5 and IMP6 begin a typical decay sequence.

At or near the end of ICME2(E), the S3(E) shock stands out with solar wind speed reaching almost 2000 km s⁻¹. After S3(E), two regions with strongly depressed temperature, considering the expected value for normally expanding solar

wind (Richardson & Cane 1995), are shown in Figure 5. The first region labeled ICME3(E) appears to be a compact, fast transient that envelops Earth for a few hours. Apparently, this transient did not intercept Pioneer 9; rather, it approached Earth from the central meridian or slightly west thereof (See element 2 in Lockwood et al. 1975's Figure 11.) At Earth, the period from August 4, 23:11 UT to August 5, 02:05 UT presents a

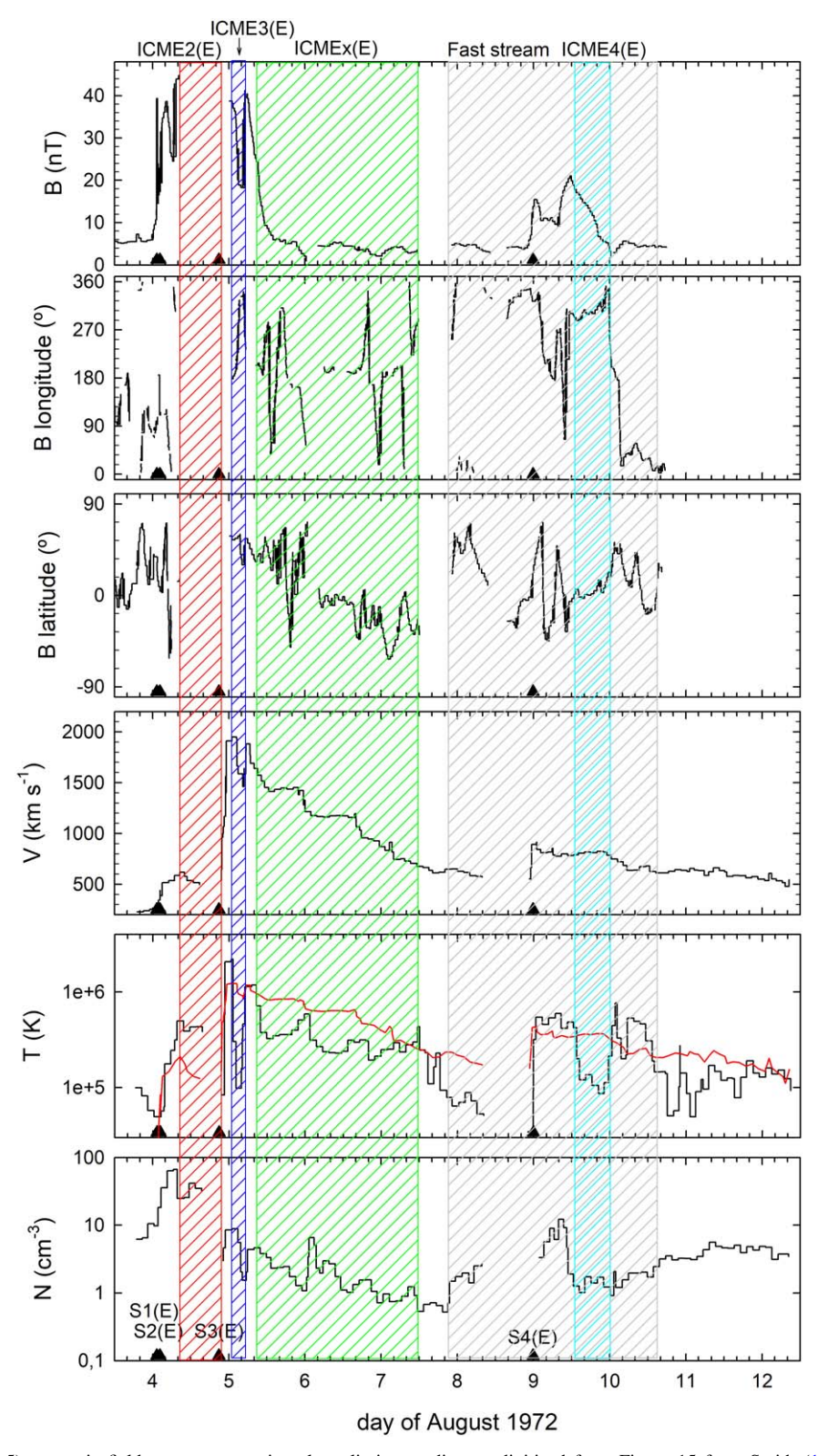


Figure 5. Explorer 41 (IMP 5) magnetic field measurements in solar-ecliptic coordinates, digitized from Figure 15 from Smith (1976), and Prognoz 2 plasma measurements during 1972 August 2–17, digitized from Figure 1 from d'Uston (1982).

smooth rotating magnetic field vector with a strength between 40 and 50 nT (d'Uston et al. 1977). The compact structure likely merged with other ejecta before reaching Pioneer 10. A complex flaring sequence in MR 11976 after 0530 UT on August 4 may have produced the closely spaced, double ejecta. There are indications from the Catania Solar Observatory that

the 06:35 UT 3B H α flare was followed within about an hour by a smaller flare (see the H α curves in Figures 3 and 4(a), (b) in Godoli & Sciuto 1973).

The second region, labeled as ICMEx(E), with a decreased temperature to values less than half of the expected one from the velocity profile (Richardson & Cane 1995), together with

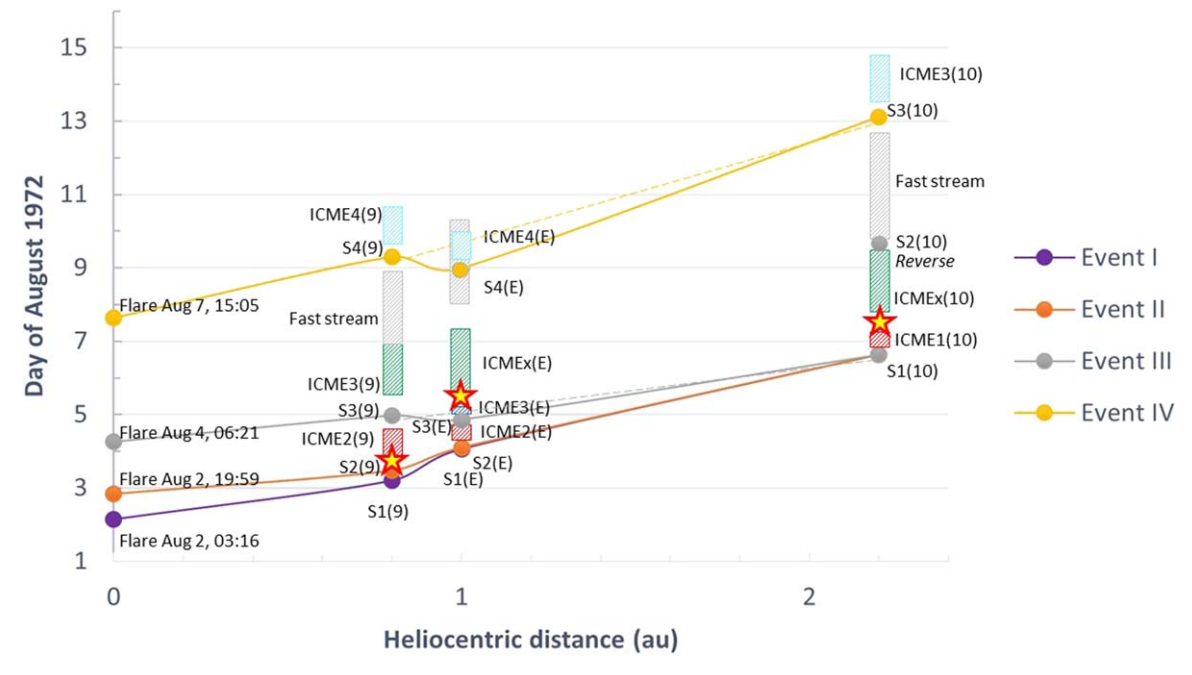


Figure 6. The events observed at different heliocentric distance from the Sun to Pioneer 10 orbit at 2.2 au. Dots correspond to the events in Table 1, and solid lines represent their association according to Dryer et al. (1975). Dashed lines indicate the radial propagation along the Sun-Pioneers line. Colored areas correspond to ICME intervals, gray areas correspond to high-speed streams, and stars indicate ICME—ICME interaction. See Section 2 for details.

the magnetic field strength close to 30 nT at the beginning of the region and a smooth rotation appearing in the magnetic field longitude, guide us to conclude that this region corresponds to ICME material. The boundaries of ICMEx(E) are fixed considering the depressed temperature time intervals and smooth and rotating magnetic field.

Solar wind speed after the ICMEx(E) interval is about 650 km s⁻¹, a too-large value for quiet solar wind. Also, the temperature reaches values of about one-third of the expected temperature from August 7, 17:12 UT until the data gap on August 8, suggesting that ICMEx(E) may extend up to \$4(4), but a new behavior in IMF appears both in latitude and longitude. Indeed, the decreased temperature is anticorrelated with an increased density, typical of interaction regions preceding the passage of a high-speed stream. About 12 hr after the shock S4(E), an interval with decreased temperature to about one-fourth of the expected value, decreased density, and enhanced, smooth magnetic field is identified as ICME4(E). After this ICME, solar wind speed slowly decreases from August 10 to August 12 from ~ 600 to ~ 500 km s⁻¹, again a speed too large for quiet solar wind. The region of the highspeed stream, shadowed in gray in Figure 5, started when temperature and density are anticorrelated and finished after the ICME4(E), when temperature departs from the expected value.

3. Assembling the IP Transients and Solar Activity

Figure 6 allow us to assemble the IP transients observed by different spacecraft and solar flares during 1972 early August. As indicated in Section 1, flares and IP shocks at different spacecraft summarized in Table 1 are shown using a dot symbol at the corresponding date and heliocentric distance, and the solid lines joining the dots indicate the assembled parts of the event proposed by Dryer et al. (1975) and supported by MHD simulations by Dryer et al. (1978). In this figure, colored areas correspond to the ICME intervals identified in Figures 3–5. Gray areas correspond to high-speed streams.

Figure 6 allow us to suggest that the CME associated with the flare on August 7 at 15:05 UT (event IV in Table 1) appears at IP medium as ICME4(9) at Pioneer 9, as ICME4(E) at 1 au, and finally as ICME3(10) at Pioneer 10 (cyan areas in Figures 3-5). This IP CME will be labeled as ICME IV from now on. In a similar way, ICME III, i.e., the CME associated with the complex flare sequence beginning about August 4 at 05:30 UT (event III in Table 1), corresponds to ICME3(9) at Pioneer 9, ICMEx(E) at 1 au and ICMEx(10) at Pioneer 10 (green areas in Figures 3–5). Regarding ICME3(E), we report it as a separate, narrow, and very fast structure at Earth, too narrow to reach Pioneer 9. After passing Earth, we suggest ICME3(E) overtook and joined with ICME2(E) to become part of the complex back side of ICME1(10). Note that the decreasing profile of solid lines of events III and IV between 0.8 au and 1 au does not indicate a deceleration of the ICMEs between 0.8 and 1 au but a faster component of the velocity in the Sun–Earth direction than the component in the Sun-Pioneer direction, evidencing a nonspherical shock waveform for the shocks associated with events III and IV as previously suggested by Zastenker et al. (1978) and Smith (1976). Dashed gray and vellow lines correspond to the propagation of events III and IV from Pioneer 9 to Pioneer 10 following the radial direction from the Sun.

Identifying ICME I and ICME II (i.e., IP counterparts of CMEs associated with events I and II in Table 1) is not an easy task as these ejections are overcome by other IP transients while traveling away from the Sun. An IP magnetic field strength over 80 nT and a proton density of about 60 cm⁻³, as recorded by Pioneer 9 on 1972 August 3, are close to the upper limits of the solar wind measurements recorded to date. Stars in Figure 6 indicate strong proton density enhancements (also magnetic strength and speed enhancement in some cases). How these parameters achieve these limits can be explained as due to a shock, S2(9), propagating inside a preceding ICME, ICME I. After the shock S2(9) has crossed the preceding ejecta, ICME I

will be stuck inside the sheath between the shock S2(9) and its driver. Indeed, simultaneous with the density spike of about 60 cm⁻³, the proton temperature is much reduced, which is uncommon within a normal sheath. Liu et al. (2020) argued that similar enhancements of magnetic field strength, solar wind speed, and density, recorded near Earth by the Wind spacecraft on 2001 November 24–25 and 2011 February 18–20 and by Stereo A spacecraft on 2012 July 23–25, represented shocked ICMEs within a disturbed sheath. That is, rather than being a part of a normal sheath region, an original, now-shocked ICME is trapped inside the sheath of a second (host) ICME.

On the contrary, proton density values of about 50 cm⁻³ measured by the ACE spacecraft on 2005 January 18 were explained by Kozyra et al. (2013) as filament material within the ICME, considering that the highest solar wind densities in ICMEs are expected to be found in solar filament material (Crooker et al. 2000). However, Kozyra et al. (2013) also mention some inconsistency in the spatial ordering of the filament material within the ICME, expected in the trailing of the ICME and not in the nose as identified, suggesting the analysis of more events with unusually dense solar wind (pointing to the 1972 August event) for definitive conclusions. Unfortunately, the limited data do not allow us to go deeper in the analysis of event I but only allow us to observe the remnants of ICME I in Pioneer 9 in a few in situ measurements (less than 7 hr of low-resolution data).

Regarding ICME II, it comes into view in Pioneer 9 as the driver of S2(9), i.e., ICME2(9), with a first interval with southward IMF followed by a similar duration interval of northward IMF. Then, at Earth, ICME2(E) is more compressed and less well sampled than at P9 but again with IMF rotating from southward to northward. The solar wind density appears high during the interval, especially at the outset. Then, Pioneer 10 measurements allow us to propose ICME1(10) as an example of the "ICME-in-sheath" phenomenon, i.e., a completely shocked ICME stuck in the sheath between a shock and a "host ejecta" (Liu et al. 2020). In situ data during the interval of ICME1(10) reveal a much larger magnetic field, speed, and density than the host ICME (in this case, ICMEx(10)), while simultaneously showing a reduced temperature. The reduced temperature is a completely anomalous behavior in a normal sheath. In conclusion, ICME II will appear as ICME2(9) at Pioneer 9, as ICME2 (E) at Earth, and will turn into an ICME in sheath in the case of ICME1(10) at Pioneer 10, i.e., red areas in Figures 3–5.

Concerning the high-speed streams, they are observed by Pioneer 9 on August 7–9 and by Pioneer 10 on August 9–13, as previously suggested by Watanabe et al. (1973) and Mihalov et al. (1974). Solar wind speed in both cases ranges between \sim 600 (at the front boundary) to \sim 400 km s⁻¹ (at the rear one). When the origin of these streams is traced to the solar corona on the assumption of constant speed and radial flow, the stream is found to originate from a well-defined EUV coronal hole that followed MR 11976 (Kakinuma & Watanabe 1976). Regarding the passage of the high-speed stream at Earth, data available do not allow us to be conclusive. However, the Earth and Pioneer 10 are almost connected by a Parker Spiral for a speed of 500 km s⁻¹, and the anticorrelation between proton temperature and density on August 8 guide us to suggest that these features correspond to the interaction region before the highspeed stream. The proposal of a high-speed stream in the vicinity of Earth on August 8 (and in the previous solar rotation) was first done by Houminer (1968). Considering the

duration of the passage of the high-speed stream at Pioneers 9 and 10, the duration of the high-speed stream at Earth is expected at least 2 days. Thus, a probable scenario includes the presence of large-scale corotating structures in the ICME IV propagation space along the heliosphere. Indeed solar wind speed is $\sim\!500~\rm km~s^{-1}$ before and after the ICME4(E). Also, after the sudden increase of magnetic field strength at S4(E) up to $\sim\!15~\rm nT$, it decreases to $\sim\!10~\rm nT$ in the sheath region and then increases again up to $\sim\!20~\rm nT$ in the ICME4(E) interval. It is not common to find a decrease of the magnetic field strength in sheaths. Winslow et al. (2021) provides an example of how interactions with corotating structures in the solar wind can induce fundamental changes in the properties of ICME sheaths.

3.1. The Radial Evolution of ICMEs

The radial alignment between Pioneers 9 and 10 during the passage of the ICMEs provides an opportunity to study the radial evolution of ICMEs using in situ measurements of the magnetic field in a similar way to the one previously done by Davies et al. (2021) with the ICME observed by Solar Orbiter on 2020 April 19 and the day after by the Wind and BepiColombo spacecraft. ICME III and ICME IV are the two candidates to focus our analysis, as two previous ICMEs turn into ICMEs-in-sheath from Pioneers 9 to 10.

When analyzing the evolution of the observed maximum and mean magnetic field strength against the heliocentric distance at each spacecraft, we observe that both magnitudes increase with the radial distance for ICME III, providing an additional signature to support the scenario of the interaction of this ICME with the previous ejections. Otherwise, magnetic field strength should decrease with heliocentric distance. For ICME IV, the mean magnetic field strength is not available as there is a data gap during that interval. Considering that the maximum magnetic field strength can be obtained from the available data, and assuming a power-law relationship passing through the two available points, we find the maximum magnetic field strength decreases with heliocentric distance as $B_{\text{max}} = 11.2d^{-1.63}$, with B in nT and d in astronomical units. The value of the exponent fully agrees with the result from Leitner et al. (2007). They obtained an exponent value of - 1.64 ± 0.40 , including in their analysis magnetic cloud data from about 0.5 to 6.5 au. Nevertheless, they indicated that for d > 2 au, the maximum magnetic field strength may decrease less rapidly than in the inner heliosphere, adding that this may be a spurious result due to poor statistics for high d. Our result indicates that the trend for the inner heliosphere still remains at least up to 2.2 au.

Using the solar wind speed time series at Pioneers 9 and 10, we can also evaluate the local expansion of the ICMEs. The dimensionless expansion parameter, ζ , (Démoulin & Dasso 2009; Gulisano et al. 2010) provides a measurement of local expansion. ζ is given by Equation (1), V_c being the cruise velocity (or the velocity at the midpoint of the ICME), d the heliocentric distance of the spacecraft, and $\frac{\Delta V}{\Delta t}$ the slope of the speed. Its physical origin is the pressure balance between the ICME and the surrounding solar wind (Démoulin & Dasso 2009):

$$\zeta = \frac{\Delta V}{\Delta t} \frac{d}{V_c^2}.$$
 (1)

For the ICME IV, we find that $\zeta = 0.80$ using speed time series at Pioneer 9 data and $\zeta = 0.78$ at Pioneer 10. The similar

results in both spacecraft agree with Gulisano et al. (2010). They proposed that for non-perturbed ICMEs, like ICME IV, ζ is confined to a narrow interval (0.91 \pm 0.23) and is independent of radial distance. Moreover, they obtained that the magnetic field strength is expected to decrease like $r^{-2\,\zeta}$. Our results also agree with this outcome.

4. Conclusions

We have analyzed the IP signatures during the 1972 early August storms through a multiset of observations identifying different ICMEs and studying their evolution from the Sun to different heliocentric distances. The result of this study allow us to identify for the first time an ICME that evolves to an "ICME in sheath," supporting the definition of this phenomenon as a completely shocked ICME stuck in the sheath between a shock and host ejecta (Liu et al. 2020). Moreover, ICME in sheath, or in a more general way, interaction between ICMEs, appears as the necessary component to achieve large values of solar wind density, magnetic field, and speed, which are the key parameters to achieve an extreme geomagnetic disturbance at Earth, as in 1972 August.

We have also studied the decrease of the maximum magnetic field strength with the heliocentric distance for a non-perturbed ICME (ICME IV). Our results conclude that the power law proposed by Leitner et al. (2007) for the inner heliosphere still remains at least up to 2.2 au. Moreover, we support that the exponent of that power law for the magnetic field is related to the parameter ζ , related to the local expansion of ICMEs, which is independent of the radial distance (Démoulin & Dasso 2009; Gulisano et al. 2010).

Acknowledgments

The research was supported by the MICINN (grant PID2020 –119407GB–I00/AEI/10.13039/501100011033) and by the University of Alcala (grant EPU–INV–UAH2021005). D.J.K. was partially supported by the Air Force Office of Scientific Research (AFOSR) award FA9550-17-1-0258 and National Science Foundation Award 1933040. We acknowledge the use of WebPlotDigitizer and data from Pioneer 10 from CDAWeb (https://cdaweb.sci.gsfc.nasa.gov/index.html/).

ORCID iDs

Consuelo Cid https://orcid.org/0000-0002-2863-3745 Elena Saiz https://orcid.org/0000-0001-7878-9476 Manuel Flores-Soriano https://orcid.org/0000-0003-2958-5949

Delores J. Knipp https://orcid.org/0000-0002-2047-5754

References

```
Burlaga, L., Sittler, E., Mariani, F., et al. 1981, JGRA, 86, 6673
Cattaneo, M., Cerulli-Irelli, P., Diodato, L., et al. 1974, in Proc. 7th ESLAB
   Symp. Vol. 42ed. D. Edgar Page (Berlin: Springer), 555
Cliver, E. W., Feynman, J., & Garrett, H. B. 1990, JGRA, 95, 17103
Coffey, H. E. 1973, Collected Data Reports on August 1972 Solar-Terrestrial
   Events UAG-28, US Dept. Commerce
Croft, T. A. 1973, JGR, 78, 3159
Crooker, N. U., Shodhan, S., Gosling, J. T., et al. 2000, GeoRL, 27, 3769
Davies, E. E., Möstl, C., Owens, M. J., et al. 2021, A&A, 656, A2
Démoulin, P., & Dasso, S. 2009, A&A, 498, 551
Dryer, M. 1975, SSRv, 17, 277
Dryer, M., Candelaria, C., Smith, Z. K., et al. 1978, JGRA, 83, 532
Dryer, M., Eviatar, A., Frohlich, A., et al. 1974, in IAU Symp. 57, Coronal
   Disturbances, ed. G. A. Newkirk (Cambridge: Cambridge Univ. Press), 377
Dryer, M., Eviatar, A., Frohlich, A., et al. 1975, JGR, 80, 2001
d'Uston, C. 1982, SSRv, 32, 99
D'Uston, C., Bosqued, J. M., Cambou, F., et al. 1977, SoPh, 51, 217
Freed, A. J., & Russell, C. T. 2014, GeoRL, 41, 6590
Godoli, G., Sciuto, V., & Zappala, R. A. 1973, Collected Data Reports on
   August 1972 Solar-Terrestrial Events, UAG-28, US Dept. Commerce
Gulisano, A. M., Démoulin, P., Dasso, S., Ruiz, M. E., & Marsch, E. 2010,
   A&A, 509, A39
Houminer, Z. 1968, Observations of Jupiter's Sporadic Radio Emission in the
   Range 7.6-41 MHz UAG-3, US Dept. Commerce
Houminer, Z., & Hewish, A. 1988, P&S
                                       SS, 36, 301
Intriligator, D. S. 1976, SSRv, 19, 629
Kakinuma, T., & Watanabe, T. 1976, SSRv, 19, 611
Knipp, D. J., Fraser, B. J., Shea, M. A., & Smart, D. F. 2018, SpWea, 16, 1635
Koehn, G. J., Desai, R. T., Davies, E. E., et al. 2022, ApJ, 941, 139
Kozyra, J. U., Manchester, W. B., IV, Escoubet, C. P., et al. 2013, JGRA,
   118, 5967
Leitner, M., Farrugia, C. J., Möstl, C., et al. 2007, JGRA, 112, A06113
Liu, Y. D., Chen, C., & Zhao, X. 2020, ApJL, 897, L11
Liu, Y. D., Luhmann, J. G., Kajdič, P., et al. 2014, NatCo, 5, 3481
Lockwood, J. A., Hsieh, L., & Quenby, J. J. 1975, JGR, 80, 1725
Mihalov, J. D., Colburn, D. S., Collard, H. R., et al. 1974, in Proc. 7th ESLAB
   Symp., Correlated Interplanetary and Magnetospheric Observations, ed.
   D. Edgar Page (Berlin: Springer), 545
Mihalov, J. D., Colburn, D. S., Smith, B. F., Sonett, C. P., & Wolfe, J. H. 1973,
   Pioneer Solar Plasma and Magnetic Field Measurements in Interplanetary
   Space During 2 August 1972, National Aeronautics and Space
   Administration
Möstl, C., Farrugia, C. J., Kilpua, E., et al. 2012, ApJ, 758, 10
Möstl, C., Weiss, A. J., Reiss, M. A., et al. 2022, ApJL, 924, L6
Richardson, I. G., & Cane, H. V. 1995, JGR, 100, 23397
Rouillard, A. P., Sheeley, N. R., Cooper, T. J., et al. 2011, ApJ, 734, 7
Salman, T. M., Winslow, R. M., & Lugaz, N. 2020, JGRA, 125,
   e2019JA027084
Smith, E. J. 1976, SSRv, 19, 661
Smith, E. J., Davis Jr., L., Coleman Jr., P. J., et al. 1977, JGR, 82, 1077
Temmer, M., & Nitta, N. 2015, SoPh, 290, 919
Tsurutani, B. T., Gonzalez, W. D., Tang, F., et al. 1992, GeoRL, 19, 1993
Watanabe, T., Kakinuma, T., Kojima, M., & Shibasaki, K. 1973, JGR,
Winslow, R. M., Scolini, C., Lugaz, N., & Galvin, A. B. 2021, ApJ, 916, 40
Zastenker, G. N., Temny, V. V., D'Uston, C., & Bosqued, J. M. 1978, JGRA,
   83, 1035
```